Decadal Variation of Rainfall Seasonality in the North American Monsoon Region and Its Potential Causes

PAOLA A. ARIAS

Department of Geological Sciences, The University of Texas at Austin, Austin, Texas, and Grupo de Ingeniería y Gestión Ambiental, Universidad de Antioquia, Medellín, Colombia

RONG FU

Department of Geological Sciences, The University of Texas at Austin, Austin, Texas

KINGTSE C. MO

Climate Prediction Center, Camp Springs, Maryland

(Manuscript received 7 March 2011, in final form 8 November 2011)

ABSTRACT

This study shows that the North American monsoon system's (NAMS) strength, onset, and retreat over northwestern Mexico exhibit multidecadal variations during the period 1948–2009. Two dry regimes, associated with late onsets, early retreats, and weaker rainfall rates, occurred in 1948–70 and 1991–2005, whereas a strong regime, associated with early onsets, late retreats, and stronger rainfall rates, occurred in 1971–90. A recovery of the monsoon strength was observed after 2005. This multidecadal variation is linked to the sea surface temperature anomalies' (SSTAs) variability, which is a combination of the Atlantic multidecadal oscillation (AMO) and the warming SST trends. These SST modes appear to cause an anomalous cyclonic circulation and enhanced rainfall over the southeastern United States and the Gulf of Mexico, which in turn increases the atmospheric stability over the monsoon region. However, these SST modes cannot fully explain the circulation and rainfall anomalies observed during the early-retreat monsoons. An expansion of the North Atlantic surface high (NASH) in recent decades also contributes to the anomalous circulation associated with the early retreats of the NAMS. A northwestward expansion of the NASH further enhances the anomalous cyclonic circulation and rainfall over the southeastern United States and the Gulf of Mexico. Its associated northwestward shift of the subtropical jets over the western United States enhances subsidence over the NAMS region. The combined effects of the AMO, the warming trends, and the NASH expansion on atmospheric circulation contribute to a stronger and more persistent earlier retreat during the recent dry regime (1991–2005), while the earlier dry regime (1948–70) appears to be only influenced by the positive phase of the AMO.

1. Introduction

The summer monsoon over the southwestern United States and Mexico, also known as the North American monsoon system (NAMS; Douglas et al. 1993; Stensrud et al. 1995), produces most of the annual rainfall in that region, where the population is growing rapidly.

Precipitation during the summer NAMS has a characteristic pattern: a precipitation maximum occurs over southwestern Mexico, although a significant area of intense precipitation is centered over northwestern Mexico; the lowest values are observed over the southwestern United States (Douglas et al. 1993; Barlow et al. 1998). The monsoon onset occurs first over southwestern Mexico by early to mid-June and rapidly progresses northward until it reaches the southwestern United States by early July (Douglas et al. 1993; Higgins et al. 1997, 1999), where rainfall is more directly influenced by midlatitude weather systems (Higgins et al. 1999). Onset of the monsoon causes a rapid change from a hot and dry weather regime to a relatively cool and rainy weather regime (Higgins et al. 1999). Observations also show that the onset of NAMS rainfall coincides with a decrease of rainfall over the Great Plains and an increase of rainfall over the eastern coast of

Corresponding author address: Paola A. Arias, Facultad de Ingenieria, Universidad de Antioquia, Medellin A.A 1226 Colombia.
E-mail: paoariasg@gmail.com

DOI: 10.1175/JCLI-D-11-00140.1

the United States (Douglas et al. 1993; Douglas and Englehart 1995; Higgins et al. 1997; Mo et al. 1997; Barlow et al. 1998).

Summer monsoon onset is a result of increasing atmospheric thermodynamic instability and moisture transport from the adjacent oceans. Higgins et al. (1997) and Adams and Comrie (1997) indicate that two main sources of moisture feed the monsoon: the northern Gulf of California provides most of the moisture below 850 hPa, while the Gulf of Mexico provides moisture at and above 850 hPa. During the monsoon period, occurrence of convection is mainly controlled by the convective inhibition (CIN) energy (Myoung and Nielsen-Gammon 2009). Evapotranspiration at land surface, local water recycling (Anderson et al. 2004; Zhu et al. 2007), and synoptic-scale transient systems (Douglas and Englehart 2007; Vera et al. 2006) also have significant influences on monsoon rainfall.

Previous studies have shown the influence of the Pacific and Atlantic SSTs on the NAMS onset and strength (e.g., Carleton et al. 1990; Harrington et al. 1992; Higgins et al. 1998, 1999; Higgins and Shi 2000, 2001; Castro et al. 2001; Zhu et al. 2007; Hu and Feng 2008, 2010; Turrent and Cavazos 2009). On the interannual scale, El Niño–Southern Oscillation (ENSO) has a strong influence on NAMS onset and rainfall amount. Wet (dry) monsoons in southwestern Mexico tend to occur during La Niña (El Niño) due to the impact of eastern Pacific sea surface temperature anomalies (SSTAs) on the land–sea thermal contrast (Higgins et al. 1999), whereas above-average July precipitation in northeastern Mexico (west-central Arizona) occurs with El Niño (La Niña) (Harrington et al. 1992). Early (late) monsoon onsets are linked to a positive (negative) thermal gradient from the Pacific to the southwestern United States during a cold (warm) phase of ENSO (Higgins and Shi 2001; Zhu et al. 2007; Turrent and Cavazos 2009). The seasonality of the Pacific SSTAs also influences NAMS. For example, Mo and Paegle (2000) have shown that warm SSTAs over the equatorial central Pacific in winter are associated with wet conditions in the southwestern United States, whereas positive SSTAs over the tropical eastern Pacific in summer lead to a drier anomaly in the same region.

On the decadal scale, several studies suggest that the variability of the NAMS is modulated by the Pacific decadal oscillation (PDO) (Higgins and Shi 2000; Castro et al. 2001, 2007), the Atlantic multidecadal oscillation (AMO), and the Arctic Oscillation (AO). For example, Hu and Feng (2008) have shown that the AMO warm phase boosts strong moisture transport from the regions near the Gulf of Mexico into the central United States, causing more rainfall over that region and less rainfall to the west and a drier monsoon. However, their study focused on the multidecadal variability of the monsoon strength but not on the associated changes in the monsoon timing. Hu and Feng (2010) have also found that the AO positive phase induces a northward displacement of the subtropical jet stream, which in turn leads to an anomalous downward motion and surface moisture divergence over the central United States, reducing precipitation in that region.

The intensity and western edge of the North Atlantic subtropical high (NASH) play an important role in determining the location and intensity of the moisture transport to the southeastern United States, and the southern and Great Plains. A recent study by Li et al. (2011) showed a westward expansion of the NASH during the summer season (June–August) since the late 1970s. This change has increased moisture transport to the Great Plains along the western edge of the NASH and rainfall variability over the southeastern and the south-central United States. However, whether these changes influence the decadal variation of the NAMS has not been investigated.

Variability of the NAMS onset and rainfall amount has been widely documented; however, variability of its retreat has received little attention. This study aims to identify whether the seasonality and strength of the NAMS have changed during the period 1948–2009 and if so, what caused such a change. This paper is organized into five sections: Section 2 describes the data and the methodology. Section 3 identifies the changes in monsoon regime and their possible causes. Finally, section 4 concludes with the main findings from this study and presents a short discussion about the main causes of the NAMS changes.

2. Data and methodology

Changes in the timing and the strength of the NAMS during the period 1948–2009 were analyzed using both daily observational and reanalysis data over the northwestern Mexico region (Fig. 1a), selected on the basis of previous studies (e.g., Barlow et al. 1998; Comrie and Glenn 1998; Higgins et al. 1999; Gutzler 2004; Gochis et al. 2006). The daily rain rate was averaged over the region and converted to mean pentad values (i.e., 5-day averages) before obtaining the onset/retreat dates.

Different definitions have been previously suggested to determine the North American monsoon onset/retreat. For example, Douglas et al. (1993) and Stensrud et al. (1995) have characterized the onset of the Mexican monsoon by analyzing heavy rainfall over southern Mexico. Douglas et al. (1993) and Barlow et al. (1998) studied the precipitation change during the Mexican

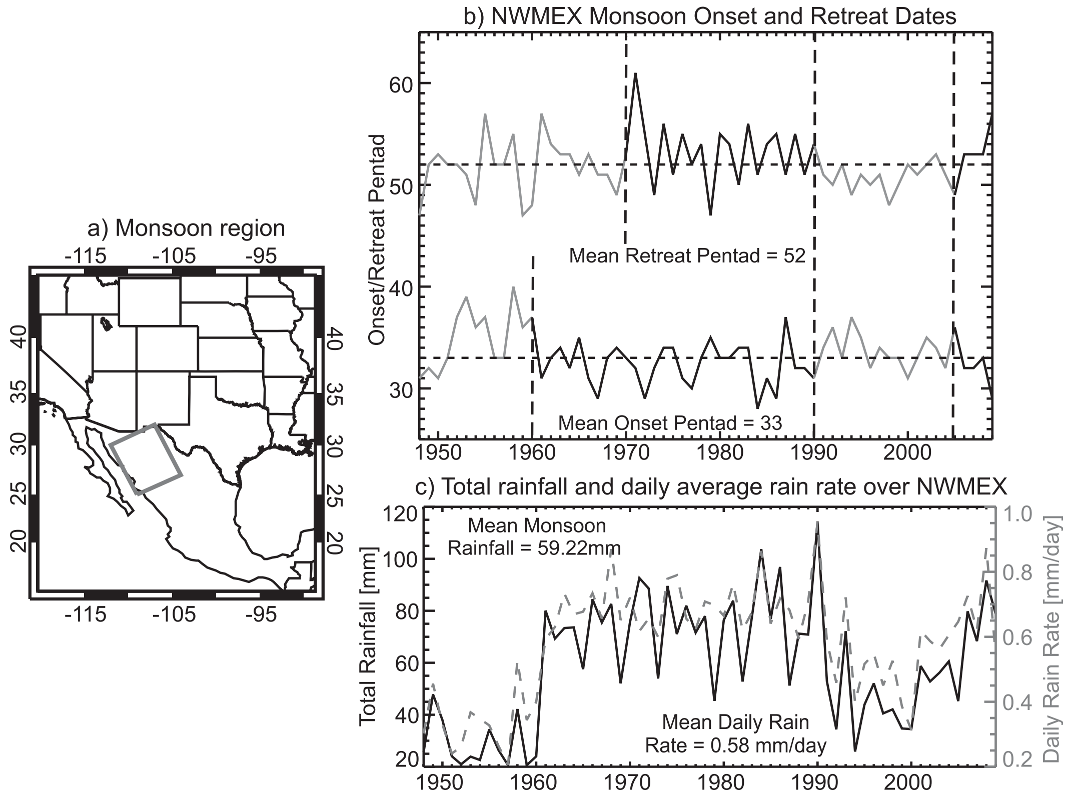

FIG. 1. (a) Monsoon region [northwestern Mexico (NWMEX)] considered for onset and retreat computations. (b) Monsoon onset (bottom line) and retreat dates (top line) over northwestern Mexico during 1948–2009 obtained from the CPC rain-rate data. Solid black lines represent periods with early onset and late retreat, whereas solid gray lines represent periods with late onset and late retreat. (c) Total rainfall (solid black line) and daily average rain rate (dashed gray line) during the entire monsoon period over northwestern Mexico. In (b), vertical dashed lines indicate the years when the monsoon regime changed, according to the STARS technique (Rodionov 2004; Rodionov and Overland 2005). Mean values during 1948–2009 are indicated in (b),(c).

monsoon onset using the June–July change. These approaches allow the main features of the onset phase to be characterized but do not identify the specific onset date. Higgins et al. (1997) used a precipitation index (i.e., the area-average daily precipitation over Arizona and western Mexico) to define the monsoon onset using a threshold-crossing procedure (with thresholds of 10.5 mm day^{-1} for rainfall and 3 days for duration). Although Higgins et al. (1997) carefully selected the grid points to be included in the area-average precipitation, their procedure considers a duration criterion of only 3 days; thus, the persistence of rainfall changes necessary for the monsoon onset may not be captured by this methodology. Zeng and Lu (2004) proposed a unified method to estimate the monsoon onset and retreat dates based on precipitable water data. Even though their results appear to be reasonable over the NAMS region, precipitable water data are available mainly from reanalysis instead of rain gauge measurements. However, monsoon retreat identification has not received as much attention as monsoon onset. Thus, the aforementioned definitions of the monsoon onset/retreat dates may have issues related to the objectivity of the rain threshold considered, the persistence in time of the rainfall changes, and/or the reliability of the required data.

Li and Fu (2004) proposed a procedure that considers both an objectively defined rain-rate threshold and the persistence in time to define the wet-season onset. Their results over South America showed consistency with previous studies. Therefore, our definition of the NAMS onset and retreat dates follows Li and Fu's methodology. The onset (retreat) date is defined as the pentad before which the rain rate is less (more) than the climatological annual mean rain rate during six out of eight preceding pentads and after which the rain rate is greater (lower) than the climatological annual mean rain rate during six out of eight subsequent pentads. When these thresholds do not allow for identifying the monsoon onset (or retreat) date for a specific year, the duration threshold is relaxed from six to five consecutive pentads. One advantage of this methodology is that long-term rain gauge data can be used instead of reanalysis products.

We used 1° grid daily precipitation across the United States and Mexico during 1948–2009 from the National Oceanic and Atmospheric Administration (NOAA)'s Climate Prediction Center (CPC). This dataset is described by Higgins et al. (1999, 2000) and is available online (ftp://ftp.cpc.ncep.noaa.gov/precip/CPC_UNI_PRCP/GAUGE_GLB/). These gridded data are collected from about 2500 gauges with hourly records across the United States and about 161 stations with daily records across Mexico (Higgins et al. 1999).

To test for changes in monsoon retreat and onset dates, a sequential *t*-test analysis of regime shifts (STARS; Rodionov 2004; Rodionov and Overland 2005) was used. This methodology uses a *t* test to determine if sequential observations in a time series represent statistically significant departures from mean values observed during the preceding period of a predetermined duration. STARS is useful for analysis toward the end of the time series, allowing for timely detection of shifts. The results are determined by the cutoff length for proposed regimes L and the Huber weight parameter H. The latter defines the range of departure from the observed mean (in standard deviations) beyond which observations are considered as outliers. In this study, L was set to 10 yr and H to 1 yr, but sensitivity analyses with L varying from 8 to 15 yr and H varying from 1 to 4 yr produced identical conclusions.

To identify the causes of the observed changes in the monsoon strength and timing, we used daily 2.5° grid data for air temperature, relative humidity, geopotential height, and zonal and meridional wind at different pressure levels. These datasets were obtained from the National Centers for Environmental Prediction–National Center for Atmospheric Research (NCEP–NCAR) reanalysis (Kalnay et al. 1996) from 1948 to 2009.

Extended reconstructed monthly-mean SST from the NOAA Climate Diagnostics Center (CDC) (Reynolds 1988) was used. The spatial resolution of the data is 2° × 2°. For the period of analysis considered here (1948–2009), the SSTs were derived from blended satellite and in situ measurements. ENSO is represented by the Niño-3 and -4 indices (available at http://www.cdc.noaa.gov/data/climateindices/list/).

We obtained composites for early- and late-retreat events to identify changes of the atmospheric fields. We defined early (late) retreat monsoon events as those when the retreat occurred before (after) the climatological retreat pentad minus (plus) one pentad. Therefore, early (late) retreats were identified as those that occurred during the period 21 August–5 September (25 September–30 October).

Changes in the monsoon regime were also examined by considering weak and strong monsoons. Weak (strong) monsoons were identified as those when the monsoon total rainfall (i.e., total amount of rainfall during the monsoon) was below (above) 0.5 standard deviations. The statistical significance of the composite difference between weak and strong monsoons was tested using a bootstrap test (Efron 1979). We performed 1000 iterations with the threshold for a statistical significance set to 95% and used the bias-corrected and accelerated percentile method to estimate the confidence interval.

A two-sample Kolmogorov–Smirnov (KS) test (Kolmogorov 1933) was performed to determine if the monsoon daily rain rate during early-retreat, late-retreat, weak, and strong monsoons exhibit different probability distributions. Because of its sensitivity to differences in both location and shape of the empirical cumulative distribution functions of the two samples, this test is one of the most useful and general nonparametric methods for comparing two samples.

Finally, to determine whether the monsoon regime changes are linked to global SSTs, we used the rotated empirical orthogonal functions (REOFs) and their associated principal components (RPCs) of the September global SSTAs during 1948–2009, as proposed by Schubert et al. (2009).

3. Results

a. *Identification of two types of monsoon regimes during 1948–2009*

Grantz et al. (2007) found that there is a significant delay in the beginning, peak, and closing stages of the monsoon over the southwestern United States during the period 1948–2004. This shift in the monsoon over this region is found to be linked to warmer tropical Pacific SSTs and cooler northern Pacific SSTs in the antecedent winter–spring season, which leads to wetter-than-normal conditions over the southwestern United States and, consequently, delays the seasonal heating of the North American continent, which is necessary to establish the monsoonal land–sea thermal contrast. In addition, previous studies suggest that northwestern Mexico exhibits a coherent hydroclimatic structure with known (and unknown) linkages to external forcing influences (e.g., Barlow et al. 1998; Comrie and Glenn 1998; Higgins et al. 1999; Gutzler 2004; Gochis et al. 2006). Hence, this work will focus on the northwestern Mexico domain of the NAMS, as shown in Fig. 1a.

The onset/retreat dates over northwestern Mexico were obtained for each year using the methodology described in section 2 and are shown in Fig. 1b. The sequential analysis STARS (Rodionov 2004; Rodionov and Overland

TABLE 1. Retreat dates over northwestern Mexico during 1948–2009 from the CPC rain-rate data. Retreat date is identified using a criterion that considers both an objectively defined rain-rate threshold and persistence throughout time following Li and Fu (2004) (see section 2). Dates in boldface (italic) correspond to early (late)-retreat events. The climatological retreat during 1948–2009 corresponds to 15 Sep. Number of early-retreat (ER) and late-retreat (LR) events with respect to the total number of years during each period is indicated in the bottom rows of each column. Cold (C) and warm (W) ENSO events are also indicated.

Year	Retreat date	Year	Retreat date	Year	Retreat date	Year	Retreat date
1948	**21 Aug**	*1971*	*30 Oct (C)*	1991	10 Sep	2006	20 Sep
1949	15 Sep	*1972*	*30 Sep (W)*	**1992**	**5 Sep**	2007	20 Sep
1950	20 Sep	**1973**	**31 Aug (C)**	1993	15 Sep	2008	20 Sep
1951	15 Sep	*1974*	*5 Oct (C)*	**1994**	**31 Aug (W)**	*2009*	*10 Oct*
1952	15 Sep	1975	10 Sep	1995	10 Sep		
1953	10 Sep	*1976*	*30 Sep (C)*	**1996**	**5 Sep**		
1954	**26 Aug (C)**	1977	15 Sep	1997	10 Sep		
1955	*10 Oct (C)*	*1978*	*25 Sep*	**1998**	**26 Aug (C)**		
1956	15 Sep	**1979**	**21 Aug**	**1999**	**5 Sep (C)**		
1957	15 Sep	*1980*	*30 Sep*	2000	15 Sep		
1958	*30 Sep*	*1981*	*25 Sep*	2001	10 Sep		
1959	**21 Aug**	**1982**	**5 Sep**	2002	15 Sep		
1960	**26 Aug**	*1983*	*5 Oct*	2003	20 Sep		
1961	*10 Oct*	1984	10 Sep	2004	10 Sep		
1962	*25 Sep (C)*	*1985*	*25 Sep (C)*	**2005**	**31 Aug**		
1963	20 Sep	*1986*	*30 Sep (C)*				
1964	20 Sep	1987	10 Sep				
1965	10 Sep	*1988*	*30 Sep (C)*				
1966	20 Sep	1989	10 Sep				
1967	10 Sep	*1990*	*25 Sep*				
1968	10 Sep						
1969	**31 Aug**						
1970	20 Sep						
No. ER	5/23		3/20		6/15		0/4
No. LR	4/23		12/20		0/15		1/4

2005) identified shifts in monsoon retreat during 1971, 1991, and 2006, whereas shifts in monsoon onset were identified during 1966, 1991, and 2006. A simple running-mean-based analysis (not shown) supports the shifts identified using STARS. This suggests that both monsoon onset and retreat exhibit multidecadal variations: more late-onset and early-retreat monsoons occurred during the periods 1948–70 and 1991–2005, whereas more early-onset and late-retreat monsoons occurred during 1971–90 and 2006–09. On the interannual scale, early-onset events are associated with late-retreat events, while late-onset events are associated with early-retreat events. The monsoon retreat dates over northwestern Mexico during 1948–2009 are shown in Table 1. The climatological mean retreat over the entire period of analysis corresponds to pentad 52 (i.e., 15 September), whereas the mean onset corresponds to pentad 33 (i.e., 12 June). Following Gutzler (2004), early (late) retreats were identified as those that occurred during the period 21 August–5 September (25 September–30 October). Early (late)-retreat events are shown in boldface (italic) in Table 1. The frequency of early-retreat and late-retreat events is specified for each period. A higher frequency of early-retreat monsoons over northwestern Mexico is observed during the periods 1948–70 and 1991–2005, although a more persistent regime of early retreats is observed during the latter period (6 early-retreat events and 0 late-retreat events out of a total of 15 events). In contrast, late-retreat monsoons are mainly observed during 1971–90 (12 events out of a total of 20 events), when retreat dates have higher variability. During the most recent period (2006–09), only one event was identified as late retreat, whereas zero early-retreat events occurred.

b. Anomalous regional rainfall patterns and related environmental conditions associated with monsoon regime changes

To identify the changes in the monsoon precipitation associated with variations in the monsoon timing, we compared the monsoon total rainfall and daily average rain rate over northwestern Mexico with the monsoon onset and retreat dates (Fig. 1c). Annual monsoon total rainfall was obtained as the total rainfall accumulated between the onset and retreat dates for each year, whereas the daily average rain rate corresponds to the daily rain rate averaged between the onset and retreat dates. Results indicate periods of dry monsoons over northwestern Mexico during 1948–70 and 1991–2005, consistent with the observed late-onset and early-retreat monsoons. Wetter monsoon periods occur during 1971–90 and 2006–09 in association with early-onset and late-retreat monsoons. Correlations between monsoon total rainfall and onset and retreat dates support this association (-0.58 and 0.6, respectively, both significant at the 1% level).

To understand the effects of the shifts in the monsoon strength over northwestern Mexico on the onset and retreat dates over the entire monsoon region, we computed the difference in onset/retreat dates between weak and strong monsoons. This difference was obtained from 21 weak monsoon and 25 strong monsoon events selected according to the criteria described in section 1. Results suggest that a weakening of the summer monsoon over northwestern Mexico is associated with a later monsoon onset (Fig. 2a) and an earlier retreat (Fig. 2b). In addition, changes in the monsoon retreat associated with variations in the monsoon strength occur over the entire NAMS domain, whereas changes in the monsoon onset are more constrained to northwestern Mexico.

To examine the association between changes in the spatial pattern of the anomalous monsoon precipitation and the variations in the monsoon strength, monsoon total precipitation anomalies and daily average monsoon rain rate were composited for early and late retreats and their difference was tested using the bootstrap test (Efron 1979). The latter was computed as the daily rain rate averaged during the entire monsoon. Anomalies were computed based on the 1948–2009 climatology. The difference composite was obtained from 14 early-retreat events and 17 late-retreat events selected according to the criteria described in section 1 and as indicated in Table 1. Figures 2c and 2d show the change in monsoonal total precipitation anomalies and daily average monsoon rain rate, respectively. Early retreats are associated with reduced precipitation over the monsoon region and increased rainfall over the central United States, not only during the entire monsoon but also in their average daily rain rate. This out-of-phase relationship between rainfall over the central United States and the monsoon region has been extensively documented (e.g., Douglas et al. 1993; Douglas and Englehart 1995; Mo et al. 1997; Higgins et al. 1997; Barlow et al. 1998). Thus, our result indicates that the early-retreat events are weaker than the late-retreat events.

To determine if the probability distributions of the daily average monsoon rain rate for early- and late-retreat monsoons (weak and strong monsoons, respectively) are statistically different, we performed a two-sample KS test (see section 2). Figure 3 shows the density functions of daily average monsoon rain rate for early-retreat, late-retreat, weak, and strong monsoons. Values in parentheses indicate the number of samples for each case. The two-sample KS test suggests that the probability distribution for early retreats (weak monsoons) is statistically different from that for late retreats (strong monsoons) at $P < 5\%$. These density functions suggest that the early-retreat/weak monsoons are associated with a reduced frequency of rainfall events, mainly of medium intensity (between 2 and 10 mm day^{-1}), and an increased frequency of weaker rainfall events (less than 2 mm day^{-1}).

Summer rainfall over the NAMS region is mainly controlled by moisture transport into the region and convective instability (e.g., Higgins et al. 1997; Adams and Comrie 1997; Anderson et al. 2004; Zhu et al. 2007). Thus, we first examined the relationship between changes of CIN, convective available potential energy (CAPE), surface dewpoint depression, and vertically integrated net moisture transport averaged over northwestern Mexico during September 1948–2009, when most of NAMS retreats occurred (Fig. 4). Following Myoung and Nielsen-Gammon (2010), we used the difference between 700-hPa temperature and surface dewpoint temperature as a proxy for CIN and the difference between surface temperature and 500-hPa temperature as a proxy for CAPE. The net moisture transport was integrated between the surface and 600 hPa. Figure 4 suggests that the multidecadal variations of the moisture transport and atmospheric stability variables generally agree with that of the monsoon retreat, as shown by their correspondent 10-yr running mean. However, correlations between these variables and the monsoon retreat date indicate that the early retreats appear to be more correlated with an increase of thermodynamic stability (CIN and CAPE) rather than with a reduction of moisture transport. An increased land surface temperature in the NAMS region would reduce surface air relative humidity, which in turn would increase CIN, reduce CAPE, and suppress monsoon rainfall.

c. *Associated changes of atmospheric circulation and sea surface temperatures*

To identify variations in the lower- and upper-troposphere circulation and sea surface temperatures associated with changes in the monsoon retreat, mean atmospheric field anomalies, daily rain-rate anomalies, and SSTAs in September were composited for early and late retreats. September composites were selected since the mean early-retreat date is 31 August and the mean late-retreat date is 5 October. Therefore, September anomalies could give insights for the observed changes of monsoon retreat.

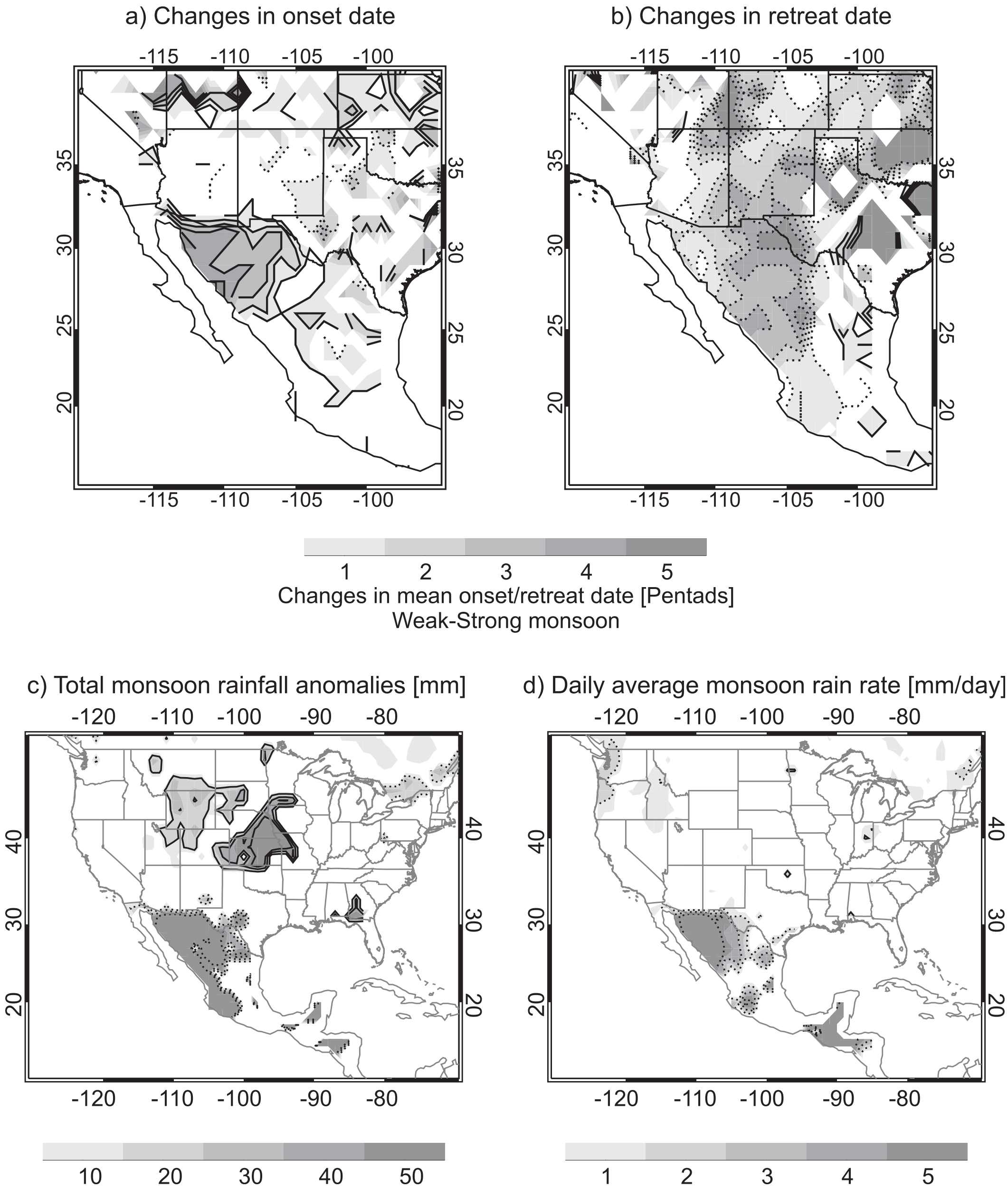

FIG. 2. Changes of (a) onset and (b) retreat dates over the southwestern United States and Mexico between weak and strong monsoons. Composite difference between weak and strong monsoons for (c) total monsoon precipitation anomalies and (d) daily average monsoon rain rate. Differences are statistically significant according to a bootstrap test (Efron 1979). Dotted (solid) contours indicate negative (positive) changes. The gray scale indicates magnitude of change.

1) Variations of lower-troposphere circulation

Figure 5 shows the mean September 850-hPa surface circulation during early and late retreats. Results suggest that the early retreats are characterized by a clearly defined cyclonic center over the Gulf of Mexico and the southeastern United States and an anticyclonic center over Baja California. These circulation anomalies are associated with the positive rainfall anomalies over the southeastern United States and negative rain-rate anomalies over the NAMS region (i.e., most of Mexico and the southwestern United States). The latter is consistent with the increase of atmospheric stability shown in Fig. 4 and contributes to an earlier retreat of the monsoon over northwestern Mexico. In addition, the earlier retreats of

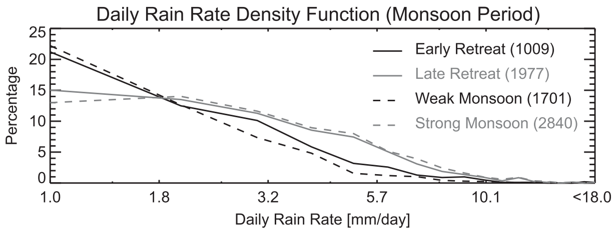

FIG. 3. Density function (%) of the daily rain rate during the monsoon for early-retreat (solid black), late-retreat (solid gray), weak monsoon (dashed black), and strong monsoon (dashed gray) events. The total number of days within the monsoon for each case is indicated in parentheses. The bin size used to compute the density function was 0.5 mm day^{-1}. The daily rain rate is plotted in logarithmic scale for a better visualization. The probability distributions are statistically different at $P < 5\%$ according to a two-sample KS test (Kolmogorov 1933).

the NAMS are also associated with an enhancement of the NASH anticyclone. In contrast, the late-retreat monsoons are associated with an anticyclonic center over the Gulf of Mexico and stronger westerly anomalies from the Gulf of California and an anomalous cyclonic circulation over Mexico, which would strengthen the monsoon and delay its retreat.

2) Variations of upper-troposphere circulation

To identify the changes of the upper-troposphere circulation between the early and the late retreats of the NAMS, Figs. 6a and 6b show the 200-hPa divergence anomalies and 200-hPa geopotential height anomalies composited during both cases. Results indicate that the early retreats are associated with anomalous upper-level divergence and increased 200-hPa geopotential height over the southeastern United States, as well as with negative 200-hPa geopotential height anomalies over the southwestern United States and northern Mexico. Furthermore, Figs. 6c and 6d show the 200-hPa zonal wind anomalies composited during early and late retreats, respectively. The anomalous upper-troposphere zonal winds suggest that the early retreats are also associated with a northwestward displacement of the subtropical jets over western North America. Hu and Feng (2010) show that a northward shift of the westerly jet stream during the positive phase of the AO produces subsidence motion and enhanced low-level divergence over the central United States. The upper-troposphere circulation composited during the early retreats (Fig. 6a) indicates enhanced upper-troposphere convergence over the central United States and northwestern Mexico, which would be consistent with enhanced lower-troposphere divergence and subsidence motion. The latter would contribute to rainfall reductions over these regions and to an earlier retreat of the NAMS over northwestern Mexico.

3) Connection to changes of sea surface temperatures

Figure 7 shows the mean September SSTAs correspondent to the four monsoon regimes identified by STARS. The first period (1948–70), characterized by more early-retreat/weak monsoons than late-retreat/strong monsoons, shows positive SSTAs over the northern Atlantic and the northwestern Pacific and negative SSTAs elsewhere. By contrast, the period 1991–2005, also identified as a regime with an enhanced frequency of early-retreat monsoons, shows warm SSTAs over the entire global oceans. In contrast, the period 1971–90,

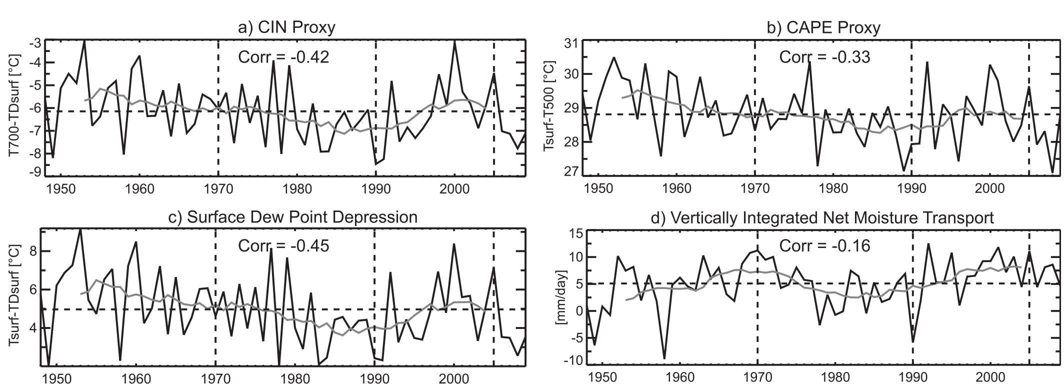

FIG. 4. NAMS domain average (solid black line) and 10-yr running mean (solid gray line) (a) CIN proxy, (b) CAPE proxy, (c) surface dewpoint depression, and (d) vertically integrated net moisture transport during September 1948–2009. Dashed lines represent the years with monsoon regime change identified by STARS (Rodionov 2004; Rodionov and Overland 2005). Correspondent correlation coefficients with NAMS retreat dates are shown in each panel.

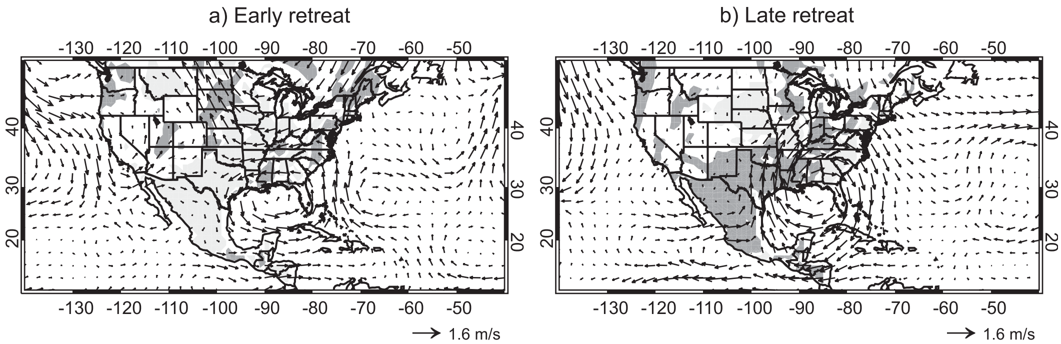

FIG. 5. September mean 850-hPa wind anomaly (arrows) and rain-rate anomaly (shading) composites for (a) early- and (b) late-NAMS-retreat events during 1948–2009. The vector scale is shown in the bottom-right corner of each panel. Dark (light) shades represent positive (negative) rain-rate anomalies.

identified as a regime with an enhanced frequency of late-retreat/strong monsoons, is associated with negative SSTAs over the North Atlantic and the North Pacific Oceans. The latter period (2005/06), when only one late-retreat event and zero early-retreat events are observed, shows warm SSTAs over the global oceans, except over the northeastern Pacific. In general, warm SSTAs over the North Atlantic are associated with early retreats, whereas cold SSTAs are associated with late retreats. These results indicate that the link between North Atlantic SSTAs and monsoon retreat holds during most of the regime epochs identified by STARS, except during the latter period. Furthermore, correlation coefficients with the September AMO index (Table 2) indicate that both monsoon strength and retreat significantly correlate at decadal scale with the AMO index but only monsoon strength also correlates at interannual scale. However, Figs. 7c and 7d clearly show that a global warming trend emerges after 1990.

To identify the main variability modes of the September SSTAs, we used the three first REOFs and their associated RPCs of the September global SSTAs during 1948–2009 (Fig. 8). The three first leading patterns are associated with the warming trends, the ENSO mode,

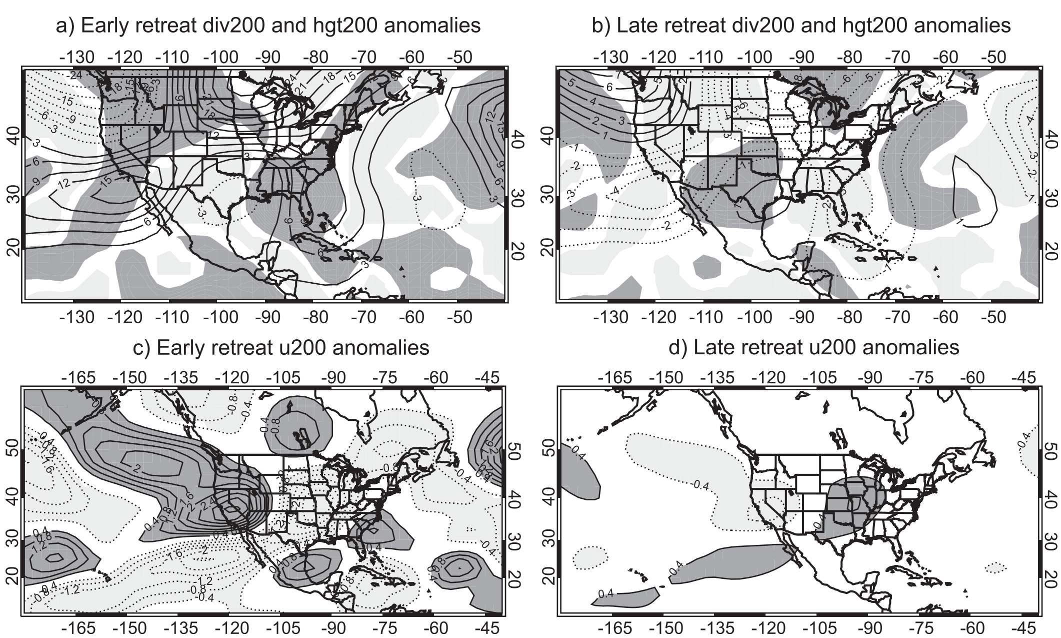

FIG. 6. September mean 200-hPa divergence anomaly (shading) and 200-hPa geopotential height anomaly (contours) composites for (a) early- and (b) late-NAMS-retreat events during 1948–2009. Solid (dotted) contours represent positive (negative) geopotential height anomalies (m). Dark (light) shades represent upper-tropospheric divergence (convergence). (c),(d) As in (a),(b), but for 200-hPa zonal wind anomalies. Solid (dotted) contours represent positive (negative) zonal wind anomalies (m s^{-1}).

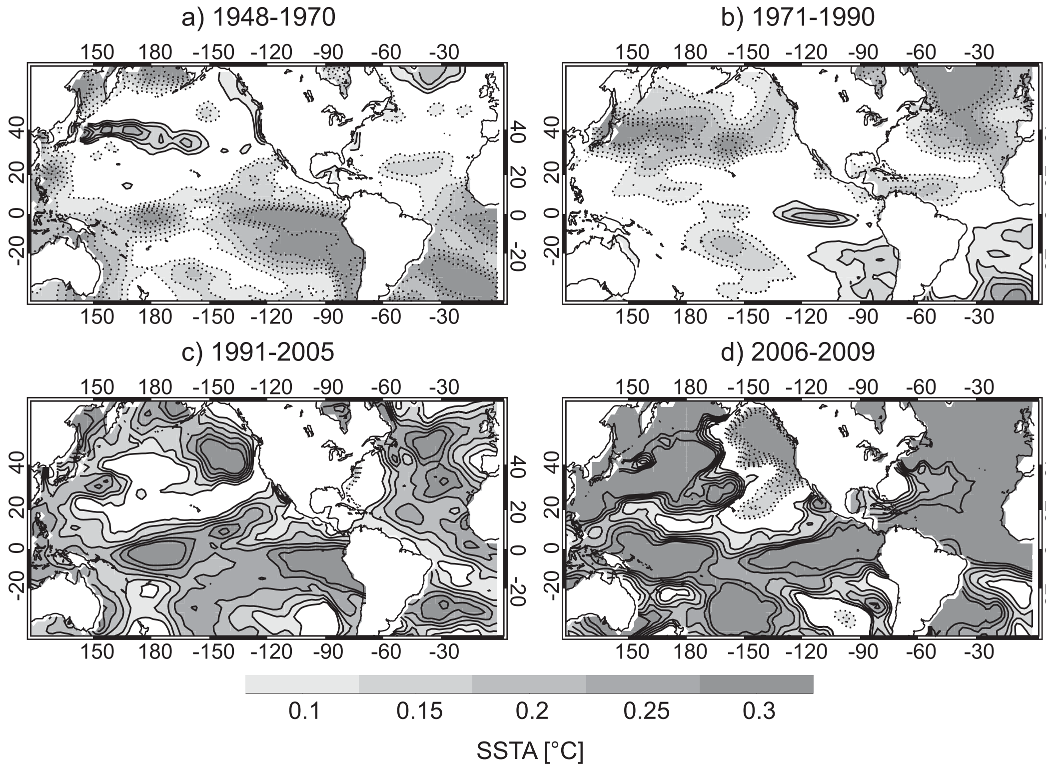

FIG. 7. September mean SSTA composites for (a) 1948–70, (b) 1971–90, (c) 1991–2005, and (d) 2006–09. Solid (dotted) contours represent positive (negative) anomalies, and the gray scale indicates their magnitude.

and the AMO mode, respectively (Figs. 8a, 8b, and 8c). These patterns are the same used by Schubert et al. (2009) in their analysis of the response of global climate models to drought-related SST patterns. Both RPC1 and RPC3 (Figs. 8d and 8f, respectively) contribute to the SSTAs in the North Atlantic. Therefore, the North Atlantic SSTAs can be viewed as the combination between the warming trends (RPC1) and the AMO mode (RPC3). This suggests that the monsoon retreat could be associated with these two modes. In contrast, the influence of the ENSO mode is not clear. Table 1 shows that eight late-retreat events and four early-retreat cases occurred during cold ENSO events. Furthermore, the interannual and decadal correlations between total monsoon rainfall (monsoon retreat date) and September ENSO indices (Table 2) suggest that the NAMS strength is only significantly correlated at decadal scale with eastern Pacific SSTAs (i.e., Niño-3 index), whereas the monsoon retreat does not significantly correlate with ENSO at any scale.

To isolate the effects of the warming trends and the AMO mode on monsoon retreat, we composited based on the events when the RPC1 and RPC3 time series, respectively, were higher than 0.5 standard deviations. Figures 9a and 9b show the composite patterns for September 850-hPa wind anomalies and rain-rate anomalies. The surface circulation anomalies associated with both modes over the monsoon region are similar to those observed during the early-retreat events (Fig. 5a). However, the warming trends and AMO mode cannot adequately explain the anomalous cyclonic circulation over the southeastern United States and the Gulf of Mexico associated with the NAMS early retreats. In contrast, the negative (positive) rain-rate anomalies over northwestern Mexico (the central and the southeastern United States) observed during the early retreats are more closely

TABLE 2. Interannual and decadal scale (i.e., using 10-yr running mean time series) correlation coefficients between total monsoon rainfall/monsoon retreat date and September AMO, Niño-3, and Niño-4 indices during 1948–2009.

	Total monsoon rainfall		Monsoon retreat date	
	Interannual	Decadal	Interannual	Decadal
AMO	−0.51*	−0.86*	−0.18	−0.75*
Niño-3	−0.07	0.34**	−0.10	0.24
Niño-4	−0.04	−0.07	−0.10	−0.20

* Correlation coefficients that are significant at $p < 1\%$.
** Correlation coefficients that are significant at $p < 5\%$.

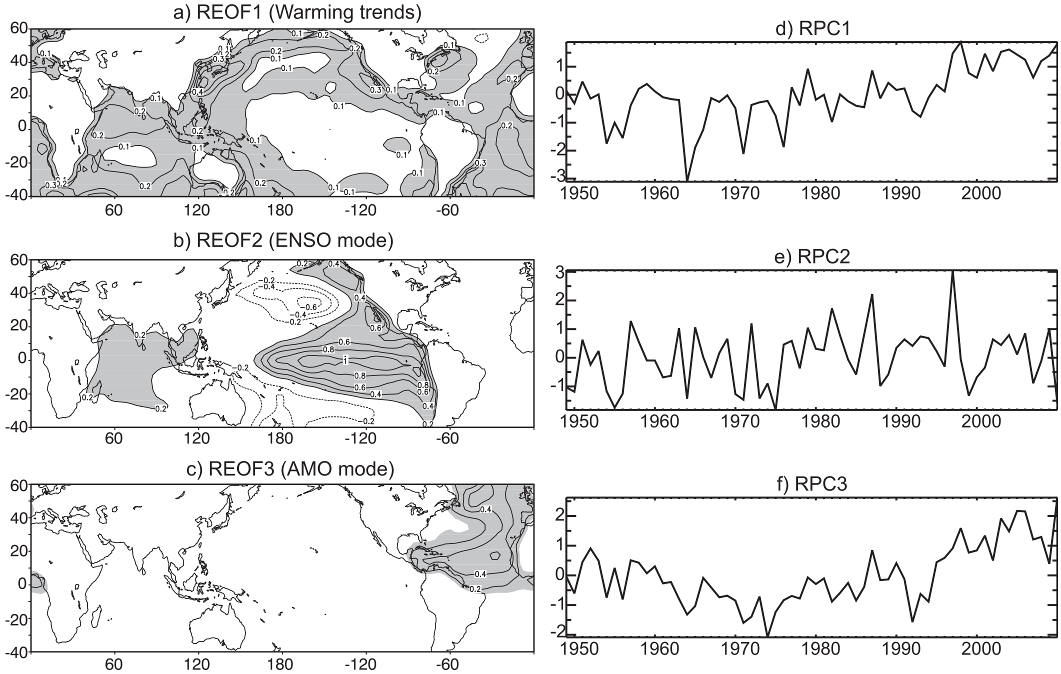

FIG. 8. First three REOFs and their associated RPCs of the September global SSTAs during 1948–2009: (a),(d) REOF 1 and RPC1 (warming trends); (b),(e) REOF 2 and RPC2 (ENSO mode); and (c),(f) REOF 3 and RPC3 (AMO mode).

resembled by the AMO mode. The correspondent composites of surface temperature anomalies and surface dewpoint depression (Fig. 10) indicate that both modes are associated with warmer surface temperatures over the monsoon region than over the south-central and the southeastern United States, especially for the warming trends.

Furthermore, the composites for upper-troposphere divergence and geopotential height anomalies (Figs. 11a and 11b, respectively) suggest that the warming trends and the AMO mode do not explain the upper-troposphere anomalous circulation (Fig. 6a) observed during the early retreats of the NAMS. However, the warming trends partially resemble the northwestward shift of subtropical jets over western North America (Fig. 12a). Therefore, our results suggest that the SST warming and AMO mode cannot fully explain the circulation changes that occurred during the NAMS early retreats.

Which other source of influence could have contributed to the observed changes in the NAMS regime in addition to that associated with the Atlantic SSTs variability? A recent study by Li et al. (2011) documents increased summer rainfall anomalies over the southeastern United States since the late 1970s in association with an intensification and a westward expansion of the western edge of the NASH (cf. Katz et al. 2003). Furthermore, their study indicates that latitudinal shifts of the NASH also affect the summer rainfall variability of the southeastern United States. However, whether these changes of the NASH western edge location could influence the strength and retreat phase of the monsoon over northwestern Mexico has not been addressed before.

The surface circulation anomalies composited during the early retreat monsoons (Fig. 5a) suggest an enhanced and more northwestwardly oriented NASH anticyclone. To further address the possible influence of this shift of the NASH western ridge on the NAMS retreat, we followed the approach of Li et al. (2011) and used the mean position of the 1560 m of geopotential height (gpm) line to characterize the western ridge of the NASH. A northwestward shift was identified when the mean September NASH western edge was located northward of 30°N and westward of 90°W (i.e., mean September latitudinal and longitudinal location of the NASH during the early retreat events). Thus, we chose 28 yr with a northwestward location of the mean September NASH western ridge during 1948–2009.

The composites for surface circulation and rain-rate anomalies based on a northwestward expansion of the NASH (Fig. 9c) indicate that such an expansion is associated with the anomalous cyclone located over the Gulf of Mexico, observed during the early-retreat events, although surface wind anomalies over northwestern Mexico cannot explain the anomalous westerly winds

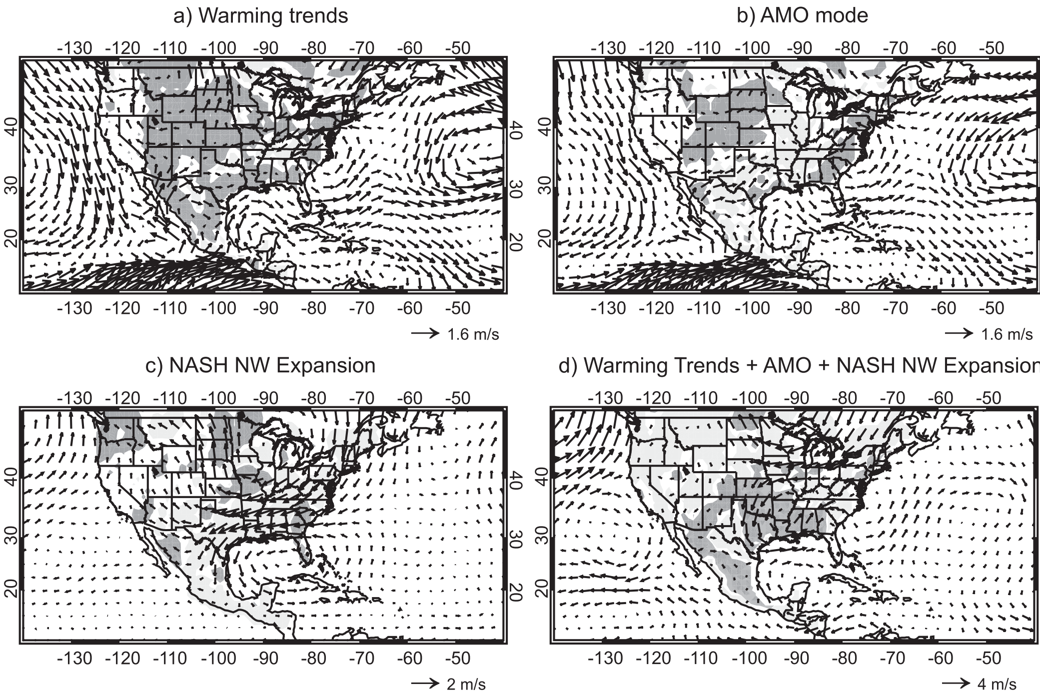

FIG. 9. September mean rain-rate anomaly (shading) and 850-hPa wind anomaly (vectors) composites for the events with (a) warming trends, (b) AMO mode, (c) NASH northwestern expansion, and (d) warming trends + AMO + NASH northwestern expansion during 1948–2009. The vector scale is shown in the bottom-right corner of each panel. Dark (light) contours represent positive (negative) rain-rate anomalies.

associated with early NAMS retreats. The latter appears to be associated with the SST warming and AMO mode (Figs. 9a and 9b). Furthermore, the upper-troposphere circulation anomalies associated with this expansion (Figs. 11c and 12c) resemble those during the early retreats more closely that the warming trends and the AMO mode.

These results indicate that the circulation pattern associated with early NAMS retreats in northwestern Mexico is probably a combined result of SST anomalies associated with the positive AMO mode and the global-scale SST warming trends, and the northwestward shift of the NASH. The former (i.e., the two SST modes) contribute to westerly anomalous wind and anticyclonic circulation in the lower troposphere, and an increase of surface temperature and a decrease of surface dewpoint depression over the NAMS region. They also contribute to an increase of geopotential height in the upper troposphere over the southeastern and the south-central United States and in part to an anomalous cyclonic circulation in the lower troposphere over the southeastern United States and the Gulf of Mexico, which is associated with early NAMS retreats. However, the northwestward shift of the NASH appears to be primarily responsible for the anomalous cyclonic circulation and an increase of rainfall over the southeastern United States and the Gulf of Mexico and the northwestward shift of the subtropical jets. The former probably drives the upper-tropospheric divergence over the southeastern United States and compensational upper-tropospheric convergence and subsidence over the NAMS region, whereas the latter has been found by previous studies (e.g., Hu and Feng 2010) to cause weaker NAMS. Thus, when these three factors are combined, the reconstructed circulation and rainfall anomalies are much more in agreement with those observed during the early retreats (Figs. 9d, 11d, and 12d).

4. Conclusions and discussion

Our study found that there are two regimes of the NAMS during 1948–2009: two dry periods during 1948–70 and 1991–2005, and one wet period during 1971–90. The dry monsoon has late onset and early retreat, while the wet monsoon, in general, has early onset and late retreat. The latest period (2006–09) suggests a recovery of the monsoon strength after the dry period of 1991–2005, although only one late-retreat/strong monsoon was observed after 2006. The NAMS early retreats are associated with an anomalous cyclonic low-level flow over the Gulf of Mexico and an anomalous anticyclonic flow over Baja California as well as with increased rainfall

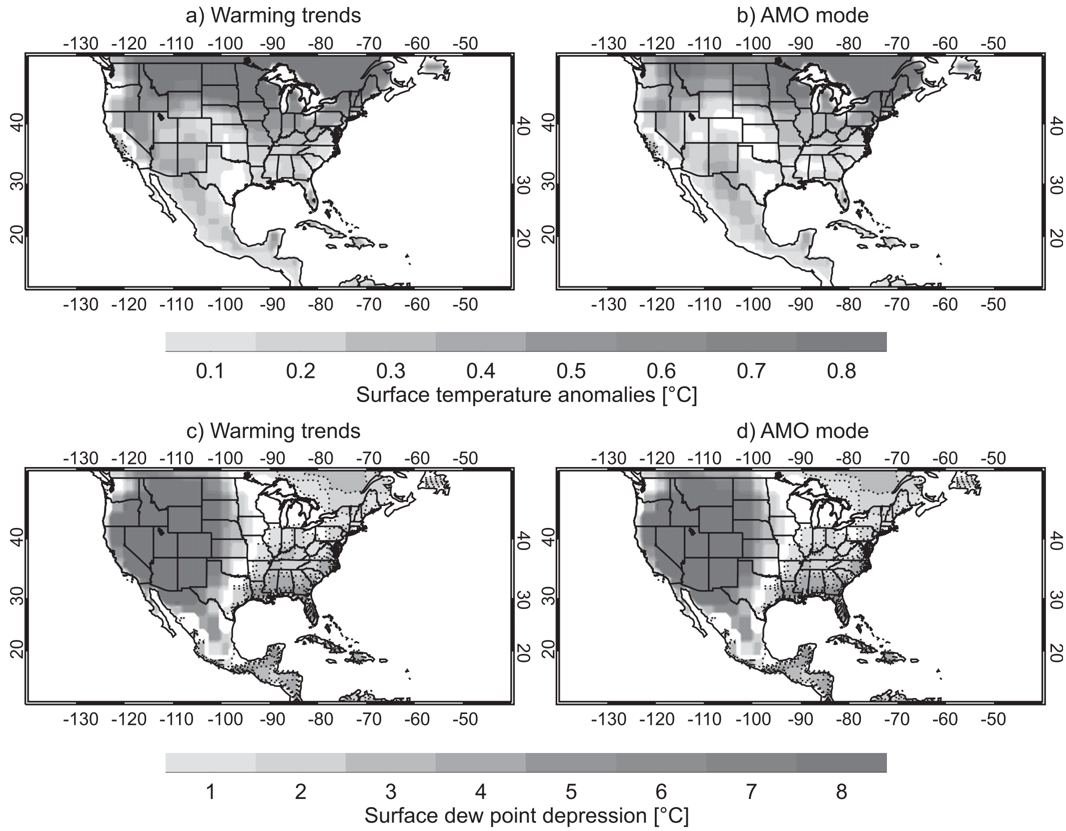

FIG. 10. September mean surface temperature anomaly composites for the events with (a) warming trends and (b) AMO mode. (c),(d) As in (a),(b), but for 850-hPa dewpoint depression. Dotted contours represent negative values, and grayscale indicates magnitude.

over the southeastern United States. These changes appear to be more related to increased atmospheric stability than to decreased moisture transport toward the monsoon region. In the upper troposphere, the early retreats are associated with anomalous divergence, increased (decreased) 200-hPa geopotential height over the southeastern United States (the southwestern United States and northern Mexico), and a northwestward displacement of the subtropical jets over western North America.

Previous studies have mainly attributed the decadal changes of the NAMS rainfall in the past several decades to ocean–atmosphere decadal variability modes, such as the PDO, the AMO, and the AO (e.g., Higgins and Shi 2000; Enfield et al. 2001; Seager et al. 2005; Schubert et al. 2004; McCabe et al. 2004; Castro et al. 2007; Hu and Feng 2008, 2010; Kushnir et al. 2010; Mo 2010). However, the changes of monsoon retreat and strength and their associated circulation anomalies reported in this study are mainly linked to the North Atlantic SSTAs variability, which can be thought of as a combination of the warming trends and the AMO mode.

The AMO mode is associated with an anomalous cyclonic circulation and enhanced rainfall over the southeastern United States. Kushnir et al. (2010) have suggested that heating anomalies resembling those during the positive AMO would induce an anomalous subsidence in the midtroposphere over the western United States and Mexico through a Gill-like response to the diabatic heating induced by warmer SSTs over the tropical Atlantic. This circulation change in turn reduces warm-season rainfall over the United States and northern Mexico. The composite circulation anomalies during the enhanced AMO mode in our Fig. 9b shows a low-level anticyclonic circulation anomaly over the NAMS region and a weakening of the NASH, which are consistent with those shown by Kushnir et al. (2010). In contrast, previous studies have attributed the recent change of the AMO to both natural AMO variability and externally forced warming (e.g., Zhang 2007; Ting et al. 2009). Thus, it is possible that the warming trends may influence the NAMS mainly through its projection onto the AMO.

Although the warming trends and the AMO mode together contribute to an enhanced subsidence over the

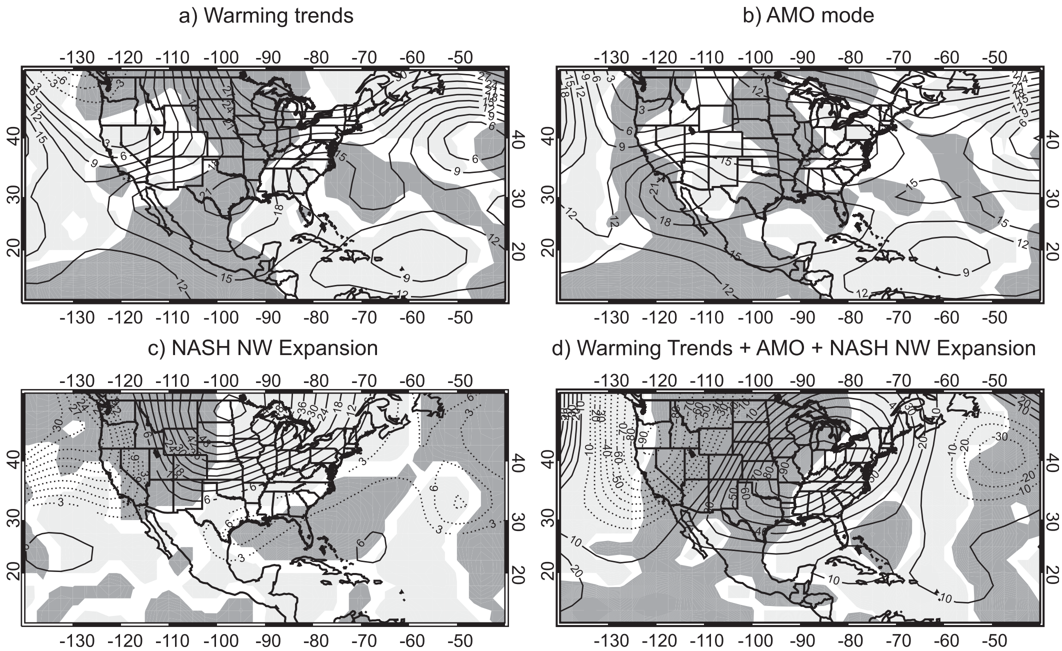

FIG. 11. As in Fig. 9, but for September mean 200-hPa divergence anomalies (shades) and 200-hPa geopotential height (contours). Solid (dotted) contours represent positive (negative) geopotential height anomalies (m). Dark (light) shades represent upper-troposphere divergence (convergence).

North American monsoon region, they cannot fully explain the circulation and rainfall anomalies observed during the early-retreat monsoons, especially the anomalous cyclonic circulation over the southeastern United States and the Gulf of Mexico and the northwestward shift of the subtropical jets over the United States. Our analysis suggests that the circulation changes are connected to the recent westward expansion of the NASH

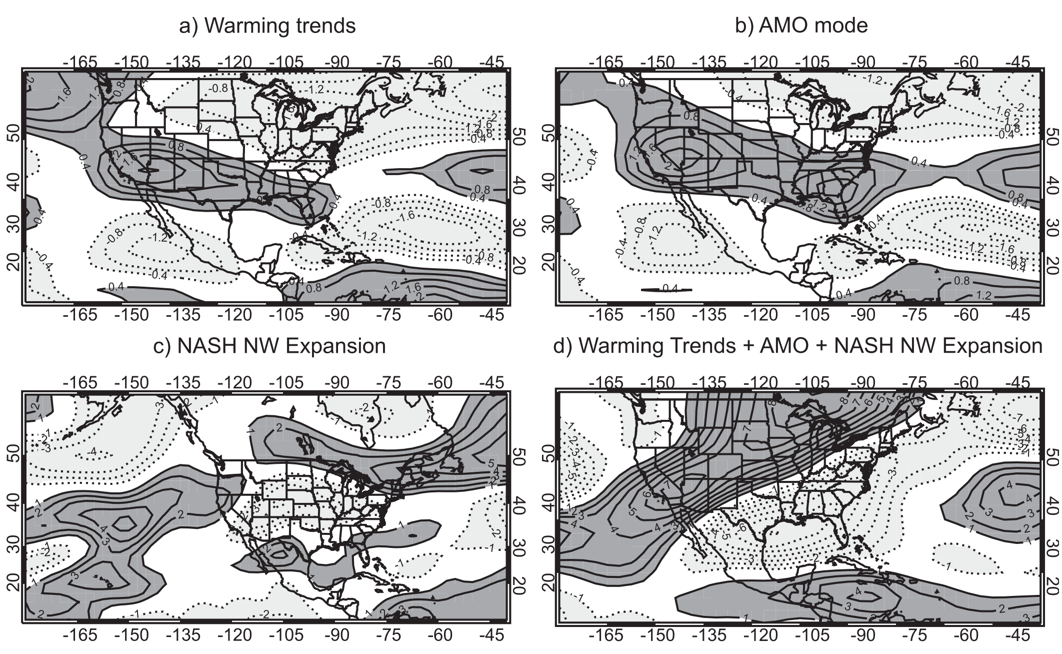

FIG. 12. As in Fig. 9, but for September mean 200-hPa zonal wind anomalies. Solid (dotted) contours represent positive (negative) zonal wind anomalies (m s^{-1}).

observed after 1978 (Li et al. 2011) and contributes to the observed NAMS changes. Such an expansion is not only associated with anomalous cyclonic circulation and enhanced rainfall over the southeastern United States and the Gulf of Mexico. The shift of the NASH western ridge also contributes to the northwestward displacement of the subtropical jets over North America. Li et al. (2011) shows that the westward expansion of the NASH is not correlated with the AMO or the PDO. Our analysis is consistent with Li et al. (2011), although these decadal SST modes could influence the intensity of the NASH, that is, its center pressure. The lack of linear correlation between the anomalous SST modes and the westward shift of the NASH is consistent with mechanisms that have been suggested by previous studies to contribute to the westward shift of the NASH. For example, Kelly and Mapes (2011) show that this westward expansion is a result of the dynamic response of zonal wind to the change of diabatic heating of the Asian monsoon. Cook et al. (2008) suggest that the westward expansion in a warmer climate is a result of stronger warming of land surface relative to that of the ocean. This change results in a shift of tropospheric air masses from the continental United States to the western Atlantic Ocean, which consequently enhances the western portion of the NASH. Our study highlights the importance of understanding the decadal variability and change of the NASH in determining the decadal variability and changes of the NAMS seasonality, a factor that was largely overlooked in previous studies.

Although this work did not address the role of the soil moisture feedback and the intraseasonal variability on atmospheric instability (and therefore on monsoon retreat), it is important to explore the influences of these processes on changes of the NAMS retreats and seasonality in our future studies.

While the observed increased occurrence of weak and early-retreat events of the NAMS is partially explained by the warming SSTAs mode, it is not clear whether the Coupled Model Intercomparison Project phase 5 (CMIP3) global climate models can adequately reproduce a weakening and an early retreat of the NAMS given the difficulty of simulating the NAMS by these models (e.g., Yang et al. 2001; Collier and Zhang 2007; Lee et al. 2007; Lin et al. 2008). The release of the CMIP5 runs would be an excellent opportunity to identify the impact of human-forced global climate change on the weakening and early retreat of the NAMS during the past few decades.

Finally, although the interannual influence of ENSO on the NAMS rainfall has also been previously documented (e.g., Harrington et al. 1992; Higgins et al. 1998, 1999), our work indicates that the observed decadal changes of the NAMS cannot be explained by an ENSO influence. However, recent model experiments by Schubert et al. (2009) and Mo et al. (2009) lead to the conclusion that the AMO modulates the impact of ENSO on seasonal drought over the United States. Thus, the contribution from the interaction between ENSO and AMO to the changes of the summer NAMS, especially during its retreat phase, is still not clear and needs further study.

Our analyses show that the combination of the warming trends, the AMO mode, and the NASH expansion produces circulation and rainfall anomalies that much closer resemble those observed during the early retreats of the monsoon. Whether the northwestward expansion of the NASH causes the associated circulation change or both are part of a planetary-scale circulation change is not clear. However, the results presented here suggest the NASH shift as a new element to be considered in understanding the mature and demise phases of the monsoon over northwestern Mexico and in improving the predictability of the NAMS decadal variability and changes.

Acknowledgments. This work was supported by the National Science Foundation (Grant AGS-0937400) and the NOAA Climate Program Office Climate Prediction Program for the Americas (CPPA) (Grant NA10OAR4310157). We sincerely appreciate the insightful suggestions from Renguang Wu, Dave Gochis, and an anonymous reviewer. We also thank Robert Dickinson and César Pastén for their help with this manuscript.

REFERENCES

Adams, D. K., and A. C. Comrie, 1997: The North American monsoon. *Bull. Amer. Meteor. Soc.,* **78,** 2197–2213.

Anderson, B. T., H. Kanamaru, and J. O. Roads, 2004: The summertime atmospheric hydrologic cycle over the southwestern United States. *J. Hydrometeor.,* **5,** 679–692.

Barlow, M., S. Nigam, and E. H. Berbery, 1998: Evolution of the North American monsoon system. *J. Climate,* **11,** 2238–2257.

Carleton, A. M., D. A. Carpenter, and P. J. Weser, 1990: Mechanisms of interannual variability of the southwest United States summer rainfall maximum. *J. Climate,* **3,** 999–1015.

Castro, C. L., T. B. McKee, and R. A. Pielke, 2001: The relationship of the North American monsoon to tropical and North Pacific sea surface temperatures as revealed by observational analyses. *J. Climate,* **14,** 4449–4473.

——, R. A. Pielke, J. O. Adegoke, S. D. Schubert, and P. J. Pegion, 2007: Investigation of the summer climate of the contiguous United States and Mexico using the Regional Atmospheric Modeling System (RAMS). Part II: Model climate variability. *J. Climate,* **20,** 3866–3887.

Collier, J. C., and G. J. Zhang, 2006: Simulation of the North American monsoon by the NCAR CCM3 and its sensitivity to convection parameterization. *J. Climate,* **19,** 2851–2866.

Comrie, A. C., and E. C. Glenn, 1998: Principal components-based regionalization of precipitation regimes across the southwest

United States and northern Mexico, with an application to monsoon precipitation variability. *Climate Res.,* **10,** 201–215.

Cook, B. I., R. L. Miller, and R. Seager, 2008: Dust and sea surface temperature forcing of the 1930's "Dust Bowl" drought. *Geophys. Res. Lett.,* **35,** L08710, doi:10.1029/2008GL033486.

Douglas, A. V., and P. J. Englehart, 1995: An analysis of the starting date for the summer monsoon in western Mexico and southeast Arizona. *Proc. 20th Annual Climate Diagnostics Workshop,* Seattle, WA, U.S. Department of Commerce, 207–211.

——, and ——, 2007: A climatological perspective of transient synoptic features during NAME 2004. *J. Climate,* **20,** 1947–1954.

Douglas, M. W., R. A. Maddox, K. Howard, and S. Reyes, 1993: The Mexican monsoon. *J. Climate,* **6,** 1665–1677.

Efron, B., 1979: Bootstrap methods: Another look at the jackknife. *Ann. Stat.,* **7,** 1–26.

Enfield, D. B., A. M. Mestas-Nuñez, and P. J. Trimble, 2001: The Atlantic multidecadal oscillation and its relationship to rainfall and river flows in the continental U.S. *Geophys. Res. Lett.,* **28,** 2077–2080.

Gochis, D. J., L. Brito-Castillo, and W. J. Shuttleworth, 2006: Hydroclimatology of the North American monsoon region in northwest Mexico. *J. Hydrol.,* **316,** 53–70.

Grantz, K., B. Rajagopalan, M. Clark, and E. Zagona, 2007: Seasonal shifts in the North American monsoon. *J. Climate,* **20,** 1923–1935.

Gutzler, D. S., 2004: An index of interannual precipitation variability in the core of the North American monsoon region. *J. Climate,* **17,** 4473–4480.

Harrington, J. A., R. S. Cerveny, and R. C. Balling, 1992: Impact of the Southern Oscillation on the North American monsoon. *Phys. Geogr.,* **13,** 318–330.

Higgins, R. W., and W. Shi, 2000: Dominant factors responsible for interannual variability of the summer monsoon in the southwestern United States. *J. Climate,* **13,** 759–776.

——, and ——, 2001: Intercomparison of the principal modes of interannual and intraseasonal variability of the North American monsoon system. *J. Climate,* **14,** 403–417.

——, Y. Yao, X. L. Wang, 1997: Influence of the North American monsoon system on the U.S. summer precipitation regime. *J. Climate,* **10,** 2600–2622.

——, K. C. Mo, and Y. Yao, 1998: Interannual variability of the U.S. summer precipitation regime with emphasis on the southwestern monsoon. *J. Climate,* **11,** 2582–2606.

——, Y. Chen, and A. V. Douglas, 1999: Interannual variability of the North American warm season precipitation regime. *J. Climate,* **12,** 653–680.

——, W. Shi, E. Yarosh, and R. Joyce, 2000: *Improved United States Precipitation Quality Control System and Analysis.* NCEP/Climate Prediction Center Atlas 7, 40 pp.

Hu, Q., and S. Feng, 2008: Variation of the North American summer monsoon regimes and the Atlantic multidecadal oscillation. *J. Climate,* **21,** 2371–2383.

——, and ——, 2010: Influence of the Arctic Oscillation on central United States summer rainfall. *J. Geophys. Res.,* **115,** D01102, doi:10.1029/2009JD011805.

Kalnay, E., and Coauthors, 1996: The NCEP/NCAR 40-Year Reanalysis Project. *Bull. Amer. Meteor. Soc.,* **77,** 437–471.

Katz, R. W., M. B. Parlange, and C. Tebaldi, 2003: Stochastic modeling of the effects of large-scale circulation on daily weather in the southeastern US. *Climatic Change,* **60,** 189–216.

Kelly, P., and B. E. Mapes, 2011: Zonal mean wind, the Indian monsoon, and July drying in the western Atlantic subtropics. *J. Geophys. Res.,* **116,** D00Q07, doi:10.1029/2010JD015405.

Kolmogorov, A. N., 1933: Sulla determinazione empirica di una legge di distribuzione. *G. Inst. Ital. Attuari,* **4,** 83–91.

Kushnir, Y., R. Seager, M. Ting, N. Naik, and J. Nakamura, 2010: Mechanisms of tropical Atlantic SST influence on North American hydroclimate variability. *J. Climate,* **23,** 5610–5628.

Lee, M.-I., and Coauthors, 2007: Sensitivity to horizontal resolution in the AGCM simulations of warm season diurnal cycle of precipitation over the United States and northern Mexico. *J. Climate,* **20,** 1862–1881.

Li, W., and R. Fu, 2004: Transition of the large-scale atmospheric and land surface conditions from the dry to the wet season over Amazonia as diagnosed by the ECMWF Re-Analysis. *J. Climate,* **17,** 2637–2651.

——, L. Li, R. Fu, Y. Deng, and H. Wang, 2011: Changes of the North Atlantic subtropical high and its role in the intensification of summer rainfall variability in the southeastern United States. *J. Climate,* **24,** 1499–1506.

Lin, J. L., B. E. Mapes, K. M. Weickmann, G. N. Kiladis, S. D. Schubert, M. J. Suarez, J. T. Bacmeister, and M. I. Lee, 2008: North American monsoon and convectively coupled equatorial waves simulated by IPCC AR4 coupled GCMs. *J. Climate,* **21,** 2919–2937.

McCabe, G. J., M. A. Palecki, and J. L. Betancourt, 2004: Pacific and Atlantic Ocean influences on multidecadal drought frequency in the United States. *Proc. Natl. Acad. Sci. USA,* **101,** 4136–4141.

Mo, K. C., 2010: Interdecadal modulation of the impact of ENSO on precipitation and temperature over the United States. *J. Climate,* **23,** 3639–3656.

——, and J. N. Paegle, 2000: Influence of sea surface temperature anomalies on the precipitation regimes over the southwest United States. *J. Climate,* **13,** 3588–3598.

——, ——, and R. W. Higgins, 1997: Atmospheric processes associated with summer floods and droughts in the central United States. *J. Climate,* **10,** 3028–3046.

——, J. E. Schemm, and S. H. Yoo, 2009: ENSO and the Atlantic multidecadal oscillation on drought over the United States. *J. Climate,* **22,** 5962–5982.

Myoung, B., and J. W. Nielsen-Gammon, 2010: Sensitivity of monthly convective precipitation to environmental conditions. *J. Climate,* **23,** 166–188.

Reynolds, R. W., 1988: A real-time global sea surface temperature analysis. *J. Climate,* **1,** 75–86.

Rodionov, S. N., 2004: A sequential algorithm for testing climate regime shifts. *Geophys. Res. Lett.,* **31,** L09204, doi:10.1029/2004GL019448.

——, and J. E. Overland, 2005: Application of a sequential regime shift detection method to the Bering Sea ecosystem. *ICES J. Mar. Sci.,* **62,** 328–332.

Schubert, S. D., M. J. Suarez, P. J. Pegion, R. D. Koster, and J. T. Bacmeister, 2004: On the cause of the 1930s dust bowl. *Science,* **303,** 1855–1859.

——, and Coauthors, 2009: A U.S. CLIVAR project to assess and compare the responses of global climate models to drought-related SST forcing patterns: Overview and results. *J. Climate,* **22,** 5251–5272.

Seager, R., N. Harnik, W. A. Robinson, Y. Kushnir, M. Ting, H. P. Huang, and J. Velez, 2005: Mechanisms of ENSO-forcing of hemispherically symmetric precipitation variability. *Quart. J. Roy. Meteor. Soc.,* **131,** 1501–1527.

Stensrud, D. J., R. L. Gall, S. L. Mullen, and K. W. Howard, 1995: Model climatology of the Mexican monsoon. *J. Climate,* **8,** 1775–1794.

Ting, M., Y. Kushnir, R. Seager, and C. Li, 2009: Forced and internal twentieth-century SST trends in the North Atlantic. *J. Climate,* **22,** 1469–1481.

Turrent, C., and T. Cavazos, 2009: Role of the land-sea thermal contrast in the interannual modulation of the North American monsoon. *Geophys. Res. Lett.,* **36,** L02808, doi:10.1029/2008GL036299.

Vera, C., and Coauthors, 2006: Toward a unified view of the American monsoon systems. *J. Climate,* **19,** 4977–5000.

Yang, Z.-L., D. Gochis, and W. J. Shuttleworth, 2001: Evaluation of the simulations of the North American monsoon in the NCAR CCM3. *Geophys. Res. Lett.,* **28,** 1211–1214.

Zeng, X., and E. Lu, 2004: Globally unified monsoon onset and retreat indexes. *J. Climate,* **17,** 2241–2248.

Zhang, R., 2007: Anticorrelated multidecadal variations between surface and subsurface tropical North Atlantic. *Geophys. Res. Lett.,* **34,** L12713, doi:10.1029/2007GL030225.

Zhu, C., T. Cavazos, and D. P. Lettenmaier, 2007: Role of antecedent land surface conditions in warm season precipitation over northwestern Mexico. *J. Climate,* **20,** 1774–1791.